12. T. Pfeiffer, S. Schuster, S. Bonhoeffer, *Science* **292**, 504 (2001).
13. C. V. Dang, G. L. Semenza, *Trends Biochem. Sci.* **24**, 68 (1999).
14. Construction and assay of the S6K1-GST construct were described previously (*22*). For the construction of the GST-ΔC-S6K1 and D3E,K100Q-S6K1-GST plasmids, similar cloning strategies were used.
15. Total RNA was isolated from HEK293 cells as described (*23*). Deacylation of tRNA was accomplished by mild alkaline hydrolysis in 0.1 M tris-HCl (pH 8.0) at 75°C for 5 min. Total RNA was electrophoresed as described (*23*), and resolved tRNA was visualized with ethidium bromide staining before being transferred to a nylon membrane by electroblotting. The individual tRNA species were probed with radiolabeled oligonucleotides as follows: for tRNALeu, 5′-GCGCCTTAGACCGCTCGGCCACG-3′; for tRNAHis, 5′-GGTGCCGTGACTCGGATTCGAACCG-3′; and for tRNAThr, 5′-GCGAGAATTGAACTCGCG-3′.
16. C. J. Lynch, H. L. Fox, T. C. Vary, L. S. Jefferson, S. R. Kimball, *J. Cell. Biochem.* **77**, 234 (2000).
17. Transiently transfected, HA-tagged mTOR from HEK293 cells was extracted after a 16-hour serum starvation and immunoprecipitated with a monoclonal antibody to HA. The immunocomplex was washed once with 1 M NaCl in assay buffer [30 mM Mops (pH 7.5), 5 mM NaF, 20 mM β-glycerol phosphate, 1 mM dithioerythritol, 0.1 % Triton X-100, and 10 % glycerol] and twice with assay buffer alone. 1 μg of a kinase-inactive, purified, soluble S6K1 substrate (S6K1-D3E,K100Q-GST) or GST-4E-BP1 was added along with assay buffer containing 10 mM $MgCl_2$ and 1 mM ATP and incubated for 30 min at 30°C. Quantitation for K_m measurements was carried out with scanning densitometry and ImageQuant software (Molecular Dynamics).
18. F. M. Gribble *et al.*, *J. Biol. Chem.* **275**, 30046 (2000).
19. A. M. Edelman, D. K. Blumenthal, E. G. Krebs, *Annu. Rev. Biochem.* **56**, 567 (1987).
20. T. Gaal, M. S. Bartlett, W. Ross, C. L. Turnbough Jr., R. L. Gourse, *Science* **278**, 2092 (1997).
21. M. Derenzini *et al.*, *J. Pathol.* **191**, 181 (2000).
22. N. Pullen *et al.*, *Science* **279**, 707 (1998).
23. J. A. Enriquez, G. Attardi, *Methods Enzymol.* **264**, 183 (1996).
24. Confluent cultures of HEK293 cells were treated as described (*9*), washed with PBS, and drained thoroughly. The cells were then scraped into 500 μl of water and sonicated with four 10-s pulses. Cell debris was removed by centrifugation, and sulfosalicylic acid was added to the supernatant to a final concentration of 2%. The samples were then placed on ice for 30 min followed by centrifugation to remove precipitated proteins. The extracts were then analyzed for amino acid content with a Biochrom 20 plus amino acid analyzer (Amersham-Pharmacia Biotech).
25. We thank W. Filipowicz, W. Krek, and M. Hall for their critical reading of the manuscript. We are also indebted to D. Cantrell for the CD2-PI3K construct, S. Schreiber for the human mTOR cDNA, and N. Pullen for the generation of a number of the S6K1 constructs used. We also thank P. Cohen and T. Hunter for useful advice with regard to the K_m of kinases for ATP. A.J. and M.S. were supported by fellowships from the Deutsche Forschungsgemeinschaft and Europen Molecular Biology Organization, and the Swiss Cancer League and the Novartis Research Foundation supported this project.

10 August 2001; accepted 10 September 2001

Dynamic Disruptions in Nuclear Envelope Architecture and Integrity Induced by HIV-1 Vpr

Carlos M. C. de Noronha,[1] Michael P. Sherman,[1,2] Harrison W. Lin,[1] Marielle V. Cavrois,[1] Robert D. Moir,[4] Robert D. Goldman,[4] Warner C. Greene[1,2,3]*

Human immunodeficiency virus–1 (HIV-1) Vpr expression halts the proliferation of human cells at or near the G_2 cell-cycle checkpoint. The transition from G_2 to mitosis is normally controlled by changes in the state of phosphorylation and subcellular compartmentalization of key cell-cycle regulatory proteins. In studies of the intracellular trafficking of these regulators, we unexpectedly found that wild-type Vpr, but not Vpr mutants impaired for G_2 arrest, induced transient, localized herniations in the nuclear envelope (NE). These herniations were associated with defects in the nuclear lamina. Intermittently, these herniations ruptured, resulting in the mixing of nuclear and cytoplasmic components. These Vpr-induced NE changes probably contribute to the observed cell-cycle arrest.

HIV-1 Vpr is a highly conserved, virion-associated (*1*), nucleocytoplasmic shuttling (*2*) protein that blocks proliferating $CD4^+$ T cells at the G_2 cell-cycle checkpoint (*3*, *4*). This property of Vpr enhances viral replication because HIV-1 transcription is more active during G_2 (*5*). Vpr also increases HIV-1 replication in nondividing macrophages, possibly by facilitating, with other viral components (*6–11*), nuclear uptake of the large (56 nm) viral preintegration complex (PIC) (*12–14*). Although Vpr has been shown to interact with various host proteins (*15–19*), the molecular mechanism underlying Vpr-induced cell-cycle arrest remains unknown.

The transition from G_2 to mitosis depends upon activation of the cyclin B1–Cdc2 kinase complex and its entry into the nucleus during prophase (*20*). The activity of Cdc2 is regulated in an opposing manner by the Cdc25C phosphatase (*21*, *22*) and the Wee1 and Myt-1 kinases (*23*, *24*). The functions of Cdc25C and Wee1 are regulated not only by changes in their overall phosphorylation but also by changes in their subcellular localization. During S phase, Cdc25C predominantly resides in the cytoplasm, reflecting its assembly with a 14-3-3 protein (*25*), whereas Wee1 is expressed in the nucleus. During prophase, both of these proteins assume a "whole cell" pattern of expression. Our initial aim was to explore whether HIV-1 Vpr alters the nucleocytoplasmic trafficking of Wee1, Cdc25C, and cyclin B1. We used video fluorescence microscopy to monitor the movement of these proteins labeled by fusion to either green or red fluorescent protein (GFP, RFP) in synchronized HeLa cell cultures cotransfected with Vpr or control expression plasmids. The dynamic changes are more readily apparent in the Web-based videos (*26*) than in the still pictures presented in the figures. When expressed alone, Wee1-GFP was observed in cell nuclei during the S and G_2 phases (Fig. 1A and Web fig. 1A). Coincident with the entry of cells into mitosis and NE breakdown, Wee1-GFP displayed a whole-cell pattern of epifluorescence (Fig. 1B and Web fig. 1A). During re-formation of the nuclear membrane in telophase, Wee1-GFP rapidly entered the daughter cell nuclei (Fig. 1, C and D, and Web fig. 1A). In the presence of Vpr, the pattern of Wee1-GFP epifluorescence was markedly different (Fig. 1, E to L, and Web fig. 1B). Notably, prominent, transient herniations formed at the apices of the oblong nuclei (Fig. 1, E to H, and Web fig. 1B). Intermittently, these herniations ruptured, releasing Wee1-GFP into the cytoplasm (Fig. 1, I to L, and Web fig. 1B). However, within 3 to 4 hours, Wee1-GFP was reimported into the nucleus (Fig. 1, K and L, and Web fig. 1B). Consistent with the cell cycle–arresting properties of Vpr, little or no mitosis was observed in these Vpr-expressing cells. Conversely, nonarresting Vpr mutants, $L^{64}QQLL/A^{64}QQAA$ (termed AQQAA) and R90K, failed to alter NE morphology, subcellular Wee1-GFP distribution, or entry into mitosis (Web fig. 2). Thus Vpr, but not nonarresting mutants of Vpr, induced dynamic herniations in the NE that intermittently ruptured.

Vpr-induced changes in intracellular trafficking of Cdc25C and cyclin B1 were also examined. Both GFP-Cdc25C and cyclin B1-GFP principally localized in the cytoplasm during the S and G_2 phases (Fig. 2, A and I,

[1]Gladstone Institute of Virology and Immunology, [2]Department of Medicine and [3]Department of Microbiology and Immunology, University of California, San Francisco, CA 94103, USA. [4]Department of Cell and Molecular Biology, Northwestern University Medical School, Chicago, IL 60611, USA.

*To whom correspondence should be addressed. E-mail: wgreene@gladstone.ucsf.edu

and Web fig. 3, A and C). At the onset of mitosis, apparently coincident with NE breakdown, Cdc25C and cyclin B1 became distributed throughout the cell (Fig. 2, B and J to L, and Web fig. 3, A and C). Cdc25C was rapidly reexported from the daughter nuclei after NE re-formation during telophase (Fig. 2, C and D, and Web fig. 3A), whereas cyclin B1-GFP fluorescence disappeared (Fig. 2L and Web fig. 3C), consistent with the reported proteasome-mediated degradation of this regulator (*27*).

In the presence of Vpr, Cdc25C and cyclin B1 localization were markedly altered. Cycles of rapid nuclear entry and exit were observed with both GFP-Cdc25C and cyclin B1-GFP during S and G_2 (Fig. 2, E to H and M to P, and Web fig. 3, B and D). Prominent nuclear herniations were also evident. In contrast to normal cells, cyclin B1-GFP was not degraded and mitosis was sharply diminished. Thus, it appears that intermittent rupture of the Vpr-induced NE herniations produced transient loss of the subcellular compartmentalization of Cdc25C, cyclin B1, and Wee1 and presumably other soluble cellular components.

These Vpr-induced NE defects and accompanying herniations were consistently observed in cells moving through S phase, indicating that these changes were not due to prolonged retention of cells in G_2. Additionally, similar nuclear herniations were not observed in cells induced to undergo G_2 arrest by exposure to mitomycin C, a DNA-damaging agent (*28*). Although Vpr has been reported to induce apoptosis, cells treated with staurosporine, a strong proapoptotic agent, did not display similar nuclear herniations (*28*).

We next explored whether structural defects in the organization of the nuclear pores or the nuclear lamina underlie the observed Vpr-induced nuclear herniations. NE herniations have been observed in yeast strains containing mutations in various nuclear pore complex (NPC) proteins (termed nucleoporins) (*29–31*). These mutations probably cause the misassembly of NPCs or defective interactions between each NPC and the surrounding "pore membrane" lipids (*30*, *31*). Nuclear export into the "dead end" structure formed by these aberrant NPCs likely fills and distends these herniations. As expected, these herniated membranes lack NPCs on their surface and do not contain DNA. Staining of Wee1-GFP and Vpr-cotransfected cells with monoclonal antibody (mAb) 414 to NPC and DNA-specific Hoechst 33342 dye (Fig. 3, D to F, and Web fig. 4) revealed that the Vpr-induced herniations (Fig. 3D and Web fig. 4, lower panels) were devoid of NPCs (Fig. 3E and Web fig. 4B, lower panel) and occasionally exhibited clustered NPCs at the base (Fig. 3E and Web fig. 4B, lower panel). However, DNA was consistently detected within these Vpr-induced NE herniations (Fig. 3F and Web fig. 4C, lower panel). Thus, although the Vpr-induced herniations exhibit certain features reminiscent of malformed NPCs, the presence of DNA in the Vpr-induced blebs argues strongly against a nucleoporin-based mechanism for the observed herniations.

Nuclear herniations have been detected in *Drosophila* (*32*), *Caenorhabditis elegans* (*33*), and mice (*34*) lacking expression of various lamin genes. In higher eukaryotes, the intermediate filament proteins lamin A, B, and C combine to form the major component of the nuclear lamina located at the inner surface of the NE. To investigate potential Vpr-induced changes in the organization of the nuclear lamina, we cotransfected HeLa cells with Wee1-RFP and GFP–lamin C in the presence or absence of Vpr. In cells lacking Vpr, lamin C accumulated at the inner surface of the nuclear perimeter, whereas Wee1 was distributed throughout the nucleus (Fig. 4A and Web fig. 5A). As cells progressed into mitosis,

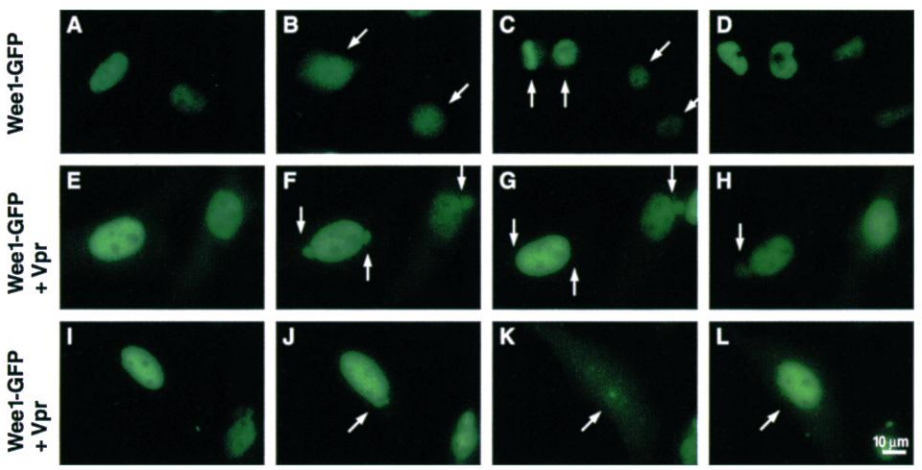

Fig. 1. HIV-1 Vpr disrupted NE architecture and integrity. (**A** to **D**) HeLa cells were cotransfected with Wee1-GFP and control expression plasmids and synchronized in the cell cycle by introduction of a double thymidine block. After removal of this block, the cells were photographed every 10 min for 20 to 24 hours. (**E** to **H**) Results of transfection of Wee1-GFP and Vpr, including NE herniations. (**I** to **L**) Rupture of a nuclear herniation. Images from various sequential time points are presented.

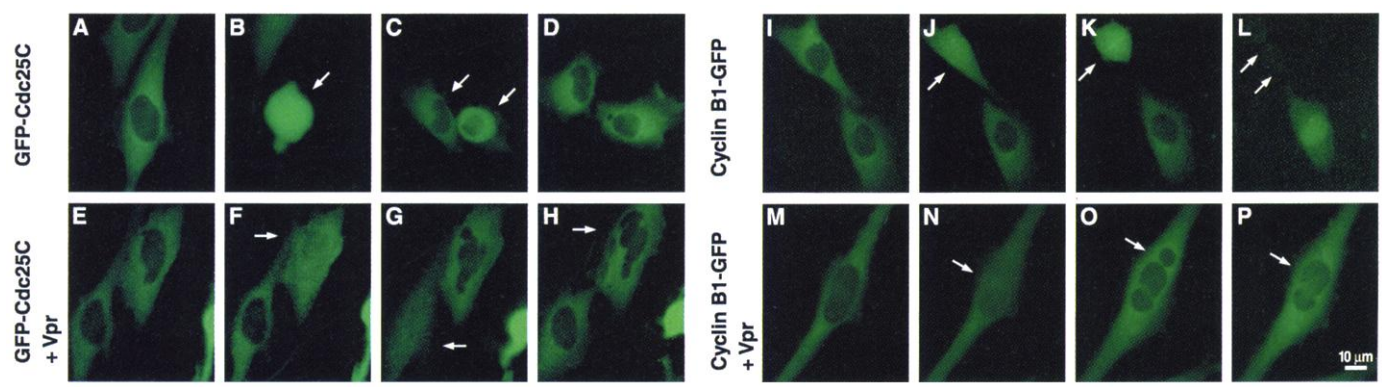

Fig. 2. HIV-1 Vpr-induced NE herniation and transient nuclear uptake of GFP-Cdc25C and cyclin B1-GFP during interphase. (**A** to **H**) Results obtained with GFP-Cdc25C in the presence (A to D) and absence of Vpr (E to H). The whole-cell pattern of GFP-Cdc25C expression is apparent in (F), followed 20 min later by a cytoplasmic pattern of expression (G). Prominent nuclear herniations are also evident in (G) and (H). (**I** to **P**) The pattern of cyclin B1-GFP expression in the presence (I to L) and absence of Vpr (M to P). (M) to (O) show images acquired over a 30-min period during S phase.

indentations in the NE appeared, followed by lamin fragmentation (Fig. 4B and Web fig. 5A). In contrast, cells expressing Vpr exhibited highly localized defects in the lamin C structure at the sites of NE herniation (Fig. 4, E to H, and Web fig. 5B). These defects in lamin C appeared as a gap in lamin C epifluorescence at the base of the nuclear herniations. In some cases, a discontinuous "flap" of lamin C was observed that moved as the herniations projected and retracted (Web fig. 5B). Vpr also induced a less uniform pattern of lamin A and B expression, producing an overall more "wrinkled" appearance (Web fig. 6, A and B, control vector versus Vpr^+). Thus, Vpr appears to induce localized disruptions in the normal nuclear lamin architecture, contributing to the formation of NE herniations.

Although Vpr is present within the herniations, this protein both accumulated at the NE, consistent with previous studies (*19*), and was more broadly distributed throughout the nucleus. We observed no evidence of increased Vpr concentration at the site of NE herniation (*28*). Thus far, a direct interaction of Vpr with the nuclear lamins A, B, or C has not been detected, raising the possibility that these effects may occur in an indirect manner. Further, we found no evidence that the Vpr-induced nuclear herniations occurred in the regions of the microtubule-organizing centers (Web fig. 7), where the NE lamina may undergo thinning and breakage as cells enter mitosis (*35–37*).

How could localized disruptions in the nuclear lamina lead to cell-cycle arrest? Defects in lamin structure are known to interfere with DNA synthesis, which in turn hinders the entry of cells into mitosis (*38*). Alternatively, the rupture of the nuclear herniations and the attendant loss of compartmentalization of key cell-cycle regulators or other cellular components may induce an intracellular injury signal that causes arrest of cells at the G_2 checkpoint.

Finally, we assessed whether HIV-1 infection produced similar morphological changes in the NE. When GHOST cells (*39*), containing an integrated HIV-1 long-terminal repeat (LTR)–GFP reporter plasmid, were infected at a high multiplicity with vesicular stomatitis virus protein G pseudotyped HIV-1, transient NE herniations were detected in both productively infected (GFP-positive) and newly infected (GFP-negative) cells (Fig. 5, A to C, and Web fig. 8). Thus, the quantities of Vpr expressed during the course of HIV infection and the levels of Vpr present in the incoming virions were sufficient to induce the observed changes in NE architecture.

Although Vpr-induced G_2 arrest increases HIV transcription, the most pronounced effects of Vpr on viral replication are observed in terminally differentiated, nondividing macrophages (*14*, *40–43*). In these macrophages, Vpr may facilitate the nuclear import of viral PICs. Notably, the 56-nm Stokes diameter (*43*) of the HIV PIC considerably exceeds the maximal 25-nm diameter of the nuclear pore channel (*44*). How the PIC successfully negotiates the NPC is unclear. It is intriguing to consider that the localized Vpr-induced NE defects may provide a portal for PIC entry into the nucleus. If Vpr facilitates nuclear uptake of the PIC through such NE defects, the quantities of Vpr present in incoming virions must be sufficient to induce these NE effects. As noted above, our studies suggest that NE herniation is evident in infected cell cultures before establishment of the HIV provirus and the production of Tat. In further support of this possibility, Vpr contained within virions has been shown to induce cell-cycle arrest (*45*, *46*). However, this potential mechanism of nuclear uptake of the PIC cannot be solely responsible for infection of nondividing cells because HIV vectors lacking Vpr can introduce genes

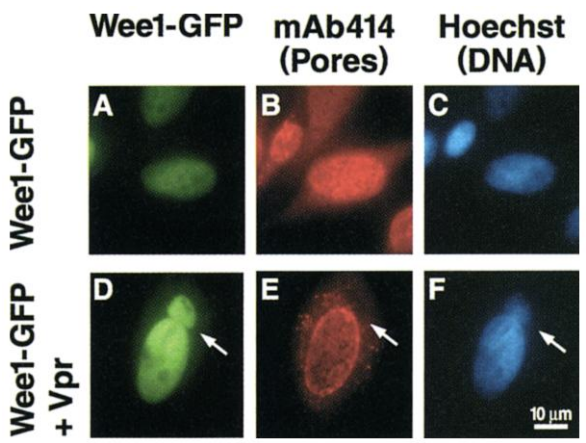

Fig. 3. Vpr-induced NE herniations are devoid of NPCs, frequently display clustered NPCs at their bases, and consistently contain DNA. HeLa cells were transfected with Wee1-GFP alone (**A** to **C**) or with Wee1-GFP and Vpr (**D** to **F**). The herniations were visualized by the presence of Wee1-GFP (D), NPCs were stained with mAb 414 to nuclear pore (B and E), and DNA was detected by staining with Hoechst 33342 dye (C and F). Arrows in (D) to (F) indicate the location of the NE herniation.

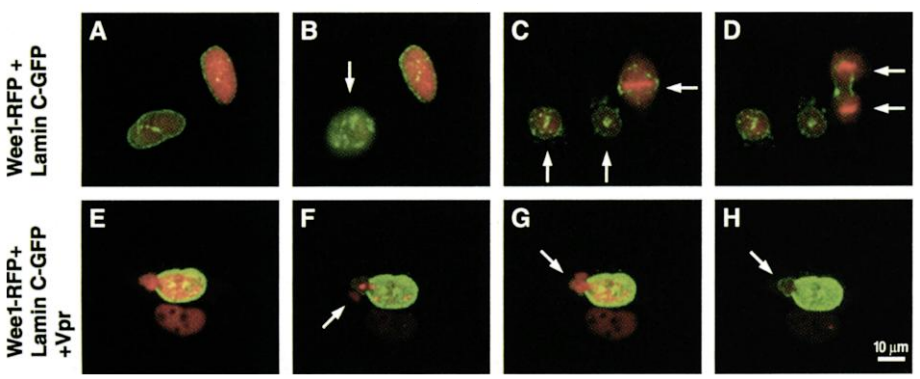

Fig. 4. HIV-1 Vpr induces localized disruptions in the nuclear lamin structure that coincide with sites of NE herniation. Synchronized HeLa cells were cotransfected with Wee1-RFP and lamin C–GFP in the absence (**A** to **D**) or presence of Vpr (**E** to **H**). The expected fragmentation of lamin C in (B) and (C) and defect in lamin C–GFP epifluorescence coincident with the site of NE herniation in (E) to (H) are indicated (arrows).

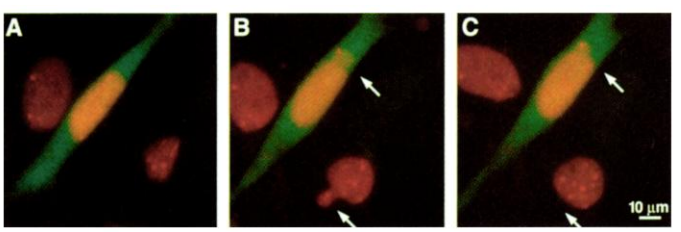

Fig. 5. (**A** to **C**) HIV infection induces nuclear herniations. HIV virions were harvested from 293T cell cultures 48 hours after cotransfection with pNL4-3 env^- Vpr^+ proviral DNA and VSV-G– and Vpr-encoding expression vectors. These pseudotyped virions were used to infect GHOST cells that contained an integrated HIV-1 LTR-GFP reporter plasmid. The images presented were acquired 17 hours after infection. NE herniation is highlighted by arrows in (B). One of these cells is productively infected by HIV, as evidenced by Tat-mediated activation of the integrated HIV-1 LTR-GFP reporter (green epifluorescence), whereas the second cell displays NE herniation at an earlier stage of infection. (C) Images acquired 20 min later, illustrating the dynamic nature of these NE abnormalities.

into various nondividing cells. Nevertheless, these effects of Vpr on nuclear lamin and NE architecture merit further evaluation in terms of their potential to facilitate HIV infection of terminally differentiated macrophages.

References and Notes

1. W. Paxton, R. I. Connor, N. R. Landau, *J. Virol.* **67**, 7229 (1993).
2. M. P. Sherman, C. M. de Noronha, M. I. Heusch, S. Greene, W. C. Greene, *J. Virol.* **75**, 1522 (2001).
3. J. B. Jowett *et al.*, *J. Virol.* **69**, 6304 (1995).
4. M. E. Rogel, L. I. Wu, M. Emerman, *J. Virol.* **69**, 882 (1995).
5. W. C. Goh *et al.*, *Nature Med.* **4**, 65 (1998).
6. U. von Schwedler, R. S. Kornbluth, D. Trono, *Proc. Natl. Acad. Sci. U.S.A.* **91**, 6992 (1994).
7. P. Gallay, V. Stitt, C. Mundy, M. Oettinger, D. Trono, *J. Virol.* **70**, 1027 (1996).
8. M. I. Bukrinsky *et al.*, *Nature* **365**, 666 (1993).
9. P. Gallay, T. Hope, D. Chin, D. Trono, *Proc. Natl. Acad. Sci. U.S.A.* **94**, 9825 (1997).
10. V. Zennou *et al.*, *Cell* **101**, 173 (2000).
11. M. Bouyac-Bertoia *et al.*, *Mol. Cell* **7**, 1025 (2001).
12. J. S. Gibbs, D. A. Regier, R. C. Desrosiers, *AIDS Res. Hum. Retroviruses* **10**, 333 (1994).
13. J. W. Balliet *et al.*, *Virology* **200**, 623 (1994).
14. N. K. Heinzinger *et al.*, *Proc. Natl. Acad. Sci. U.S.A.* **91**, 7311 (1994).
15. S. Mahalingam *et al.*, *Proc. Natl. Acad. Sci. U.S.A.* **95**, 3419 (1998).
16. A. Gragerov, T. Kino, G. Ilyina-Gragerova, G. P. Chrousos, G. N. Pavlakis, *Virology* **245**, 323 (1998).
17. Y. Refaeli, D. N. Levy, D. B. Weiner, *Proc. Natl. Acad. Sci. U.S.A.* **92**, 3621 (1995).
18. R. A. Fouchier *et al.*, *J. Virol.* **72**, 6004 (1998).
19. M. A. Vodicka, D. M. Koepp, P. A. Silver, M. Emerman, *Genes Dev.* **12**, 175 (1998).
20. J. Pines, T. Hunter, *J. Cell Biol.* **115**, 1 (1991).
21. P. Russell, P. Nurse, *Cell* **45**, 145 (1986).
22. ———, *Cell* **49**, 559 (1987).
23. Reviewed in D. J. Lew, S. Kornbluth, *Curr. Opin. Cell Biol.* **8**, 795 (1996).
24. Reviewed in T. R. Coleman, W. G. Dunphy, *Curr. Opin. Cell Biol.* **6**, 877 (1994).
25. C. Y. Peng *et al.*, *Science* **277**, 1501 (1997).
26. Supplementary Web material is available on *Science* Online at www.sciencemag.org/cgi/content/full/294/5544/1105/DC1.
27. M. Jackman, M. Firth, J. Pines, *EMBO J.* **14**, 1646. (1995).
28. C. M. de Noronha *et al.*, unpublished data.
29. U. Nehrbass, M. P. Rout, S. Maguire, G. Blobel, R. W. Wozniak, *J. Cell Biol.* **133**, 1153 (1996).
30. S. R. Wente, G. Blobel, *J. Cell Biol.* **123**, 275 (1993).
31. ———, *J. Cell Biol.* **125**, 955 (1994).
32. B. Lenz-Bohme *et al.*, *J. Cell Biol.* **137**, 1001 (1997).
33. J. Liu *et al.*, *Mol. Biol. Cell* **11**, 3937 (2000).
34. T. Sullivan *et al.*, *J. Cell Biol.* **147**, 913 (1999).
35. J. P. Stafstrom, L. A. Staehelin, *Eur. J. Cell Biol.* **34**, 179 (1984).
36. M. R. Paddy, H. Saumweber, D. A. Agard, J. W. Sedat, *J. Cell Sci.* **109**, 591 (1996).
37. M. Terasaki, *Mol. Biol. Cell* **11**, 897 (2000).
38. R. D. Moir, T. P. Spann, H. Herrmann, R. D. Goldman, *J. Cell Biol.* **149**, 1179 (2000).
39. D. Cecilia *et al.*, *J. Virol.* **72**, 6988 (1998).
40. M. I. Bukrinsky *et al.*, *Proc. Natl. Acad. Sci. U.S.A.* **89**, 6580 (1992).
41. R. I. Connor, B. K. Chen, S. Choe, N. R. Landau, *Virology* **206**, 935 (1995).
42. S. Popov *et al.*, *EMBO J.* **17**, 909 (1998).
43. M. D. Miller, C. M. Farnet, F. D. Bushman, *J. Virol.* **71**, 5382 (1997).
44. S. I. Dworetzky, C. M. Feldherr, *J. Cell Biol.* **106**, 575 (1988).
45. B. Poon, K. Grovit-Ferbas, S. A. Stewart, I. S. Chen, *Science* **281**, 266 (1998).
46. M. Hrimech, X. J. Yao, F. Bachand, N. Rougeau, E. A. Cohen, *J. Virol.* **73**, 4101 (1999).

47. We thank D. Morgan, T. Hunter, H. Piwnica-Worms, and H. Worman for the expression plasmids. We also thank R. Givens for administrative assistance and J. Carroll and S. Gonzalez for graphics assistance. This work was supported in part by NIH grant R01 AI145234 (to W.C.G.) and by core facilities provided by the UCSF–Gladstone Institute of Virology and Immunology, Center for AIDS Research, P30 MH59037. M.P.S. was supported by NIH/NIAID grant KO8 AI01866.

2 July 2001; accepted 31 August 2001

Interaction of the Response Regulator ARR4 with Phytochrome B in Modulating Red Light Signaling

Uta Sweere,[1] Klaus Eichenberg,[1] Jens Lohrmann,[1] Virtudes Mira-Rodado,[1] Isabel Bäurle,[1] Jörg Kudla,[2] Ferenc Nagy,[3] Eberhard Schäfer,[1] Klaus Harter[1]*

The *Arabidopsis thaliana* response regulator 4, expressed in response to phytochrome B action, specifically interacts with the extreme amino-terminus of the photoreceptor. The response regulator 4 stabilizes the active Pfr form of phytochrome B in yeast and in planta, thus elevates the level of the active photoreceptor in vivo. Accordingly, transgenic *Arabidopsis* plants overexpressing the response regulator 4 display hypersensitivity to red light but not to light of other wavelengths. We propose that the response regulator 4 acts as an output element of a two-component system that modulates red light signaling on the level of the phytochrome B photoreceptor.

Phytochromes (phy) are red/far-red reversible photoreceptors that regulate many aspects of plant development (*1*). They are synthesized in the dark in the inactive Pr form and converted by red light into their active far-red light–absorbing Pfr form. In *Arabidopsis* the phy family is encoded by five genes (*PHYA* to *PHYE*), whose products forward the light signal to downstream transduction components by separate signaling mechanisms (*1*, *2*). Light signal transduction is mediated by proteins that interact with phytochromes in the cytoplasm and the nucleus (*1*, *3*). The cyanobacterial phytochrome, Cph1, is a light-regulated histidine kinase (*4*), therefore it appeared conceivable that eukaryotic phytochromes may also function as sensor kinases (*5*), yet no eukaryotic phytochromes displaying histidine kinase activity have been described (*6*).

The *Arabidopsis* EST and genome databases contain several genes for plant response regulators with similarity to the *Escherichia coli* response regulator CheY (*7*, *8*). One of the identified clones was identical with the recently published *Arabidopsis* response regulator 4 (ARR4, Fig. 1A) (*9*, *10*). We generated an ARR4-specific antiserum to analyze the expression of this protein in planta. This antiserum detected the ARR4 protein in stems, leaves, and flowers but not in roots (Fig. 1B). Thus, the expression pattern of ARR4 overlaps in great part with that of phyB. The amount of ARR4 remained below detection level in seedlings grown in darkness, whereas in light, the accumulation of the protein was detectable 1 day after germination (Fig. 1C). Accumulation of ARR4 was induced by white or red light in dark-grown seedlings, whereas far-red light was ineffective (Fig. 1D). Hourly pulses of 5 min of red light given over a period of 24 hours also induced accumulation of ARR4 protein (Fig. 1D). The inductive effect of red light was reversed by a subsequent far-red light pulse (Fig. 1D). Accumulation of ARR4 was also analyzed in *Arabidopsis phyA* and *phyB* mutants. It was reduced in red light–irradiated *phyB*-mutant seedlings, but was unaffected in *phyA*-mutant (Fig. 1E). These data suggest that phyB dominates the photoregulation of ARR4 expression, although participation of other photoreceptors, especially in white light, should not be excluded.

To investigate a physical interaction of ARR4 with phyB, copurification experiments were performed. Wild-type phyB, a mutated phyB resulting in a reduced red light–sensitive phenotype [phyB-101 (*11*)], and phyA were expressed in yeast (*12*). Functional photoreceptors were obtained by self-assembly with chromophore in crude extracts and far-

[1]Institut für Biologie II / Botanik, Universität Freiburg, Schänzlestrasse 1, 79104 Freiburg, Germany. [2]Molekulare Botanik, Universität Ulm, Albert-Einstein-Allee 11, 89069 Ulm, Germany. [3]Institute of Plant Biology, Biological Research Center, P.O. Box 521, 6701 Szeged, Hungary.

*To whom correspondence should be addressed. E-mail: harterkl@uni-freiburg.de